Three-Dimensional Linear and Nonlinear Transformations: An Integration of Light Microscopical and MRI Data

Thorsten Schormann* and Karl Zilles

C. and O. Vogt Institute of Brain Research, Heinrich-Heine University Düsseldorf, Germany

Abstract: The registration of image volumes derived from different imaging modalities such as MRI, PET, SPECT, and CT has been described in numerous studies in which functional and morphological data are combined on the basis of macrostructural information. However, the exact topography of architectural details is defined by microstructural information derived from histological sections. Therefore, a technique is developed for integrating micro- and macrostructural information based on 1) a three-dimensional reconstruction of the histological volume which accounts for linear and nonlinear histological deformations, and 2) a two-step procedure which transforms these volumes to a reference coordinate system. The two-step procedure uses an extended principal axes transformation (PAT) generalized to affine transformations and a fast, automated full-multigrid method (FMG) for determining high-dimensional three-dimensional nonlinear deformations in order to account for differences in the morphology of individuals. With this technique, it is possible to define upwards of 1,000 times the resolution of ~1 mm in MRI, making possible the identification of geometric and texture features of microscopically defined brain structures. *Hum. Brain Mapping 6:339–347, 1998.*   © 1998 Wiley-Liss, Inc.

Key words: histology; MRI; registration; linear transformation; nonlinear transformation
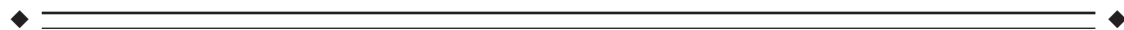
INTRODUCTION

Computerized brain atlases are commonly used for assigning functional activations to anatomical structures and for studying intersubject variability in order to make generalizations about localizations of function and structure at macroscopical and microscopical levels in different individuals. In order to interpret information derived from individual topologies, it is required to transform the volumes with highest accuracy.

The most important component of such an atlas is therefore a spatial normalization (deformation) technique in order to fit the sizes and shapes of individual brains (by deforming the volumes), and to map the volumes into one coordinate system, i.e., the standard reference system (''reference'' or ''standard'' brain [Roland and Zilles, 1994, Schormann et al., 1997]). Even microstructural information can be integrated, if the deformation algorithm transforms each individual brain data set nonlinearly, i.e., completely onto the reference brain by a recently developed full multigrid technique [Schormann et al., 1996]. In practice, this means that the technique must account for large and complex spatial differences, which can only be accomplished by high dimensional transformations derived from nonlinear deformation algorithms. From a physical and a mathematical point of view the transforma-

tion, with up to 24 million degrees of freedom, is uniquely determined since the same number of constraints is introduced by the principle of Hamilton and thus the three-dimensional deformation can be calculated precisely within a selected degree of accuracy for each voxel. From a morphological point of view, the correlation of corresponding structures in both volumes is improved by a multiresolution full-multigrid technique (FMG), whereby special attention is required in the case of pathological structures (e.g., anomalous sulcal and gyral patterns). Another advantage of the FMG technique is that the number of operations increases only linearly with the number of voxels.

A further important step toward the integration of micro- and macrostructural information is the precise three-dimensional reconstruction of the histological volume on the basis of the undistorted MR reference brain. Once the histological volume is three-dimensionally reconstructed, specific structures such as fiber tracts or borders of architectonically defined areas can be identified at microstructural resolution by using the original histological sections. Thus the MR volume and the original histological sections both show the same regions, but with a resolution improved by a factor of 1,000 provided by the histological sections. Delineation of structural entities is then performed on digitized images of the histological sections, and this information is subsequently introduced into the reference coordinate system by linear and nonlinear transformations.

DATA ACQUISITION

The MR volumes were acquired with the Magnetom SP (Siemens) at a magnetic field strength of 1.5 T. Each volume consists of a series of 128 sagittal sections which covers the entire brain and in which the contrast depends on the specific tissue parameters (proton density, T_1-, T_2-relaxation times) and on parameters of the pulse sequence (repetition time, echo time, inversion time). T_1-weighted volumes are created by a fast, low-angle shot (three-dimensional flash, flip-angle 40°) with a repetition time of TR = 40 msec and an echo time of TE = 5 msec for each image. The image space is discretized into voxels in the form of rectangular parallelepipeds of uniform size, each with a resolution of 8 bits corresponding to 256 gray values. The integer indices i, j, k denote the coordinates of the voxels and are given by: $0 \leq i \leq i_{max}$, $0 \leq j \leq j_{max}$, $0 \leq k \leq k_{max}$. In our application, i_{max}, j_{max} are 255 and k_{max} = 128. The indices may be converted to real-world coordinates X, Y, Z in object space by:

$$X = \epsilon_{ij} \cdot i; \quad Y = \epsilon_{ij} \cdot j; \quad Z = \epsilon_k \cdot k$$

in which the scaling constants ϵ are used to specify the unit dimension of the volume element in object space corresponding to a voxel in image space whereby the isotropic voxel size for MR images is given by $\epsilon_{ij}^M = 1$ mm. The voxel size in the z-direction amounts to $\epsilon_k^M = 1.17$ mm.

The paraffin-embedded brain is sectioned in the frontal plane and the Nissl-stained sections are then digitized with a CCD camera. The gray value of a voxel is then proportional to the optical density converted from the transmission signal with isotropic voxel $\epsilon_{ij}^H = 0.9$ mm. The mean thickness of a histological section is determined by $\Delta Z \sim 30$ μm, resulting in a Z-resolution of $\epsilon_k^H = 1.8$ mm, since each sixtieth section is used for three-dimensional reconstruction. In order to account for the different directions of sectioning between the MR and the histological volumes and anisotropic voxel sizes in both volumes, an affine transformation is applied which is superior to a scaling-rotation transformation for several theoretical and practical reasons [Schormann et al., 1993]. As a result, both volumes have isotropic voxel size and the same direction of sectioning (frontal), but at slightly differing angles of ~10–20° due to lack of stereotaxic fixation during data acquisition. This misalignment is corrected by a three-dimensional affine transformation, whereby the convergence to the best least-square parameters is controlled by a matrix-norm (see below).

THREE-DIMENSIONAL RECONSTRUCTION OF HISTOLOGICAL SECTIONS

In order to reconstruct the histological volume, each brain is represented by three data sets: 1) the histological data set with high contrast, but disorganized and distorted because of the preparation procedures; 2) the photo-data set with low contrast (resulting from the unstained surface of the paraffin block) showing the histological section before sectioning, together with a reference system in order to establish the three-dimensional integrity of the histological volume; and 3) an MR-data set with improved contrast but at a slightly different orientation than the photo-data set. The three-dimensional reconstruction and spatial corrections of the histological images on the basis of a photo-data set and a postmortem MR volume are required in order to take into account:

1) Linear and nonlinear deformations resulting from the histological preparation procedures;
2) Three-dimensional reconstruction of the histological images, since the information on the position of adjacent sections is lost during sectioning;

3) Different direction of sectioning between photo- and MR-data set (∼10–20°, see above).

The entire sequence of algorithms for image processing of the data sets can be described using the following sequence of techniques.

In a first step, it is required to align the photo-data set by using the reference system which is digitized in conjunction with the surface of the paraffin-embedded brain before sectioning. These images need to be aligned, since the chuck of the microtome may have different positions during data acquisition. For a precise alignment using one image of the series as reference, the images are transformed by an automated rigid least-squares transformation (rotation and translation) whereby the definition and correlation of corresponding landmarks encompassing the reference system is similar to an image processing procedure described earlier [Schormann et al., 1995]. After this processing, the three-dimensional integrity of the photo-data set is reestablished. The next step is to reconstruct the digitized histological series, which has higher contrast than the photo-data set. For this purpose, each histological section is registered with the corresponding photo by an extension of the principal axes theory generalized to affine transformations [Schormann et al., 1997]. This generalization is required, since the classical PAT cannot in principle account for affine transformation parameters [Schormann and Zilles, 1997]. Such parameters account for shearing artifacts introduced during preparation procedures. This three-dimensional reconstructed volume defines a first approximation of the histological volume. For further improvement of registration quality, the histological volume is three-dimensionally aligned with the corresponding postmortem MR-volume in a next step, whereby the convergence to the best parameters is controlled by a matrix-norm [Schormann et al., 1993], since the determination of least-squares parameters are hampered by local deformations in the histological volume. After this three-dimensional alignment, both volumes have the same direction of sectioning and can be used for a further global, linear two-dimensional refinement by analyzing Rayleigh-Bessel statistics, which describe the probability density of local nonlinear deformations [Schormann et al., 1995] in histological sections. In a last step, nonlinear deformations are corrected by the three-dimensional FMG technique (described below) restricted to two dimensions. The histological volume is then reconstructed with subvoxel accuracy and excellent contrast (Fig. 1), and can be used for identifying microstrucural features.
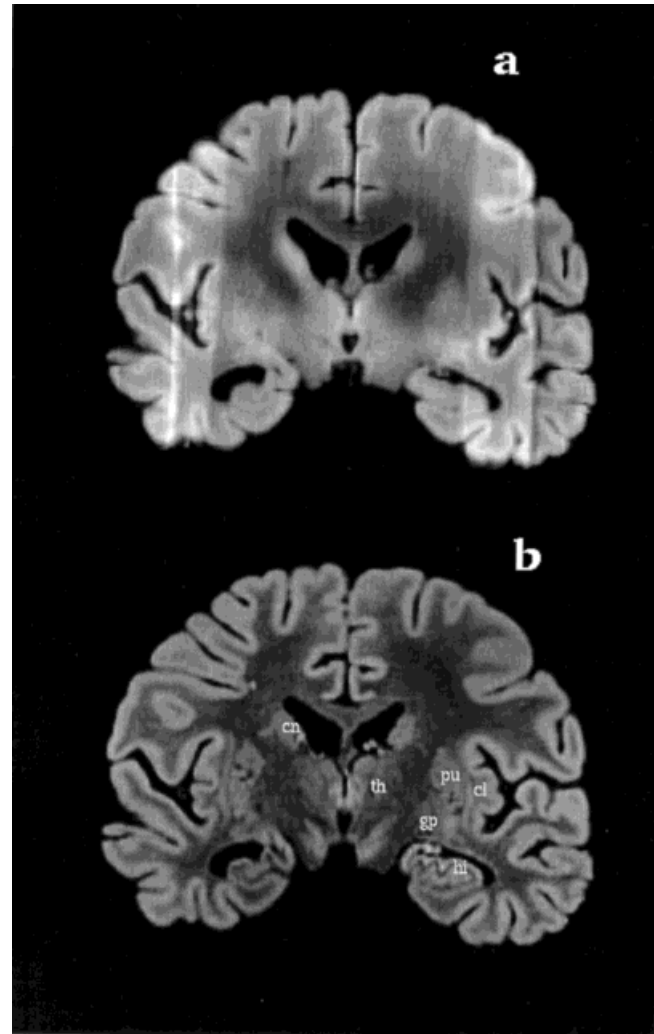

Figure 1.
Sections resulting from MR **(a)** and from the three-dimensional reconstruction of the histological volume **(b)**. As can be seen, the same direction of sectioning is achieved whereby nonlinear deformations are corrected by a two-dimensional version of the three-dimensional nonlinear model (described below) on the basis of the spatially undistorted MR reference section. The histological specimen is used for the identification of microstructural information, which can be mapped to the histological image with superior contrast. cl, claustrum; cn, caudate nucleus; gp, globus pallidus; hi, hippocampus; pu, putamen; th, thalamus.

INTERINDIVIDUAL REGISTRATION

Linear alignment

In order to study the variability of microscopically defined brain structures between individuals, it is necessary to transform the individual data sets into
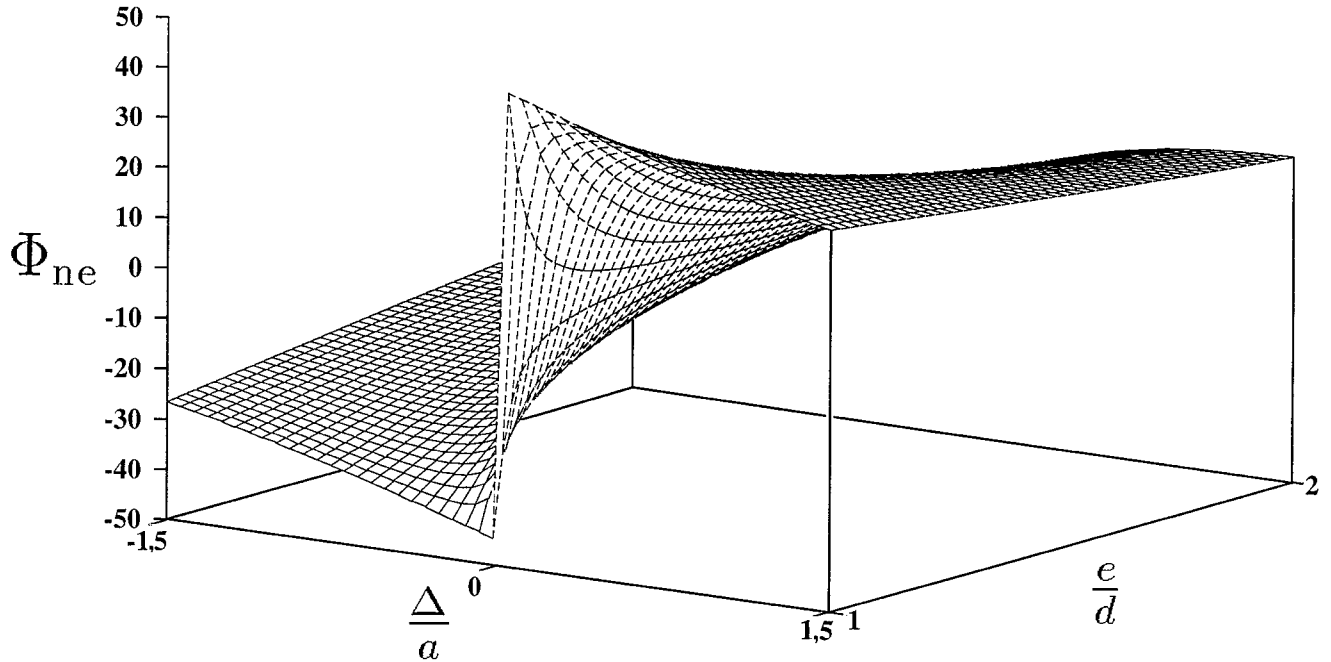
Figure 2.

Rotational error ϕ_{ne} as a function of the form factor $\frac{e}{d}$ and the shearing parameter $\frac{\Delta}{a}$ using the classical PAT. For $\frac{e}{d} = 1$, the rotational error varies from $+45°$–$-45°$ if $\pm\frac{\Delta}{a} \rightarrow 0$. This misalignment cannot be attributed to the principal axes algorithm itself, but is a consequence of its application to data which do not completely fulfill the assumption of rigid-body transformation and scaling. The errors can be avoided by application of the extended PAT.

one common coordinate system prior to nonlinear transformation, since the orientation of the reference and individual volumes differs slightly, usually by 10–20° for each direction due to lack of appropriate stereotaxic fixation during data acquisition. In addition, the data sets must be rescaled because of anisotropic resolution and the different sizes of the brains. Registration is achieved by means of an extended principal axes theory [Schormann et al., 1997] which accounts for global geometrical differences (scaling) as well as rotation and translation. Twelve parameters are therefore required to match both volumes in three dimensions: three parameters for translation, three for scaling along the three axes of the Cartesian coordinate system, and six angles which can be calculated by decomposing a three-dimensional affine transformation into a product of the forms rotation, scaling, and another rotation. Six angles are therefore needed for rotations around the three axes. Unfortunately, the classical PAT can correct at most for scaling and rotational parameters ($\frac{1}{2}n(n + 1)$ parameters in n dimensions). This is due to the symmetrical inertia matrices of the individual and reference objects. which lead to large rotational and scaling errors even for infinitesimal shearing resulting from mechanical treatment or distortion caused by the imaging system. The degree of misregistration depends on a shearing parameter $\frac{\Delta}{a}$ and a form parameter $\frac{e}{d}$ which describes the ratio of width to height of the object [Schormann and Zilles, 1997].

The rotation error is given by

$$\phi_{ne} = \frac{1}{2} \arctan\left[2\left(\frac{\Delta}{a} + \frac{a}{\Delta} \cdot \left(\frac{e^2}{d^2} - 1\right)\right)\right] \quad (1)$$

and the scaling error by

$$e_s = \frac{\left(1 + \frac{\Delta^2}{2 \cdot a^2}\right) + \sqrt{\left(1 + \frac{\Delta^2}{2 \cdot a^2}\right)^2 - 1}}{\left(u + \sqrt{u^2 - \frac{d^2}{e^2}}\right)^2}$$

with $u = \frac{1}{2}\left(1 + \frac{d^2}{e^2}\left(1 + \frac{\Delta}{a}\right)^2\right)$ \quad (2)

whereby the rotational error is shown in Figure 2.

As can be seen, minute shearing of highly symmetrical objects results in misalignment of $\sim \pm 45°$, depending on the sign of the shearing parameter in the case of the classical PAT. This misalignment cannot be attributed to the PAT itself, but is a consequence of its application to data which do not completely fulfill the assumption of rigid-body transformation and scaling. However, exact global registration is an important prerequisite for subsequent matching with nonlinear deformation techniques, since 1) global misalignment does not need to be corrected locally, and 2) the correlation of homologous structures is improved by a unique initial position for the application of a nonlinear model. This improvement is achieved by an extended PAT which is generalized to affine transformations by introducing a rotational matrix $P = (\epsilon_1, \epsilon_2, \epsilon_3)$, which parametrizes all solutions of possible affine transformations T in three dimensions according to

$$T = R_2^t J_2^{\frac{1}{2}} P J_1^{-\frac{1}{2}} R_1^t \qquad (3)$$

whereby the exact affine transformation parameters T_{exact} are calculated by independantly varying Euler angles $\epsilon_1 \in [0,\pi]$, $\epsilon_2 \in [0, +2\pi]$, $\epsilon_3 \in [0,2\pi)$ [for details see Budò, 1980] and simultaneously optimizing a similarity citerion such as the extent of overlap. In Eq. (3), t is the transpose of the matrix, R_1 denotes an eigenvector matrix which transforms the inertia matrix M_1 of the individual brain into the principal moment matrix J_1, and R_2 denotes an eigenvector matrix which transforms the inertia matrix M_2 of the reference brain into the principal moment matrix J_2 by a similarity transformation. Eq. (3) describes the determination of affine transformation parameters used in this study. See Schormann et al. [1997a] and Schormann and Zilles [1997] for a detailed discussion on the extended PAT. Translation is corrected by superposition of the centers of mass $<\vec{x}>_1$ and $<\vec{x}>_2$ of both volumes. Thus, a point $\vec{x}_1$ of the template is transformed onto the corresponding point $\vec{x}_2$ of the reference coordinate system by the relation

$$\vec{x}_2 = T_{exact}(\vec{x}_1 - <\vec{x}>_1) + <\vec{x}>_2 \qquad (4)$$

Eq. (4) has the advantage that the calculation of higher-order moments is not required and it is therefore not sensitive to noise. Moreover, there are no restrictions with respect to symmetries which pose problems for the classical PAT or PAT-based methods using odd-order moments [Faber and Stokeley, 1988; Cygansky and Orr, 1985]. After transforming the histo-logical data, both volumes have the same global orientation based on the linear transformation parameters (Fig. 1).

Nonlinear alignment

In order to account for differences in the morphology of individuals, the objects (brains) are modelled as an elastic medium by applying the theory according to Navier-Lamé [Landau and Lifshitz, 1959; Broit, 1981; Bajcsy and Kovacic, 1989; Miller et al., 1993; Christensen et al., 1994; Bro-Nielsen and Gramkow, 1996; Schormann et al., 1996]. In the present approach, investigation is focused on minimizing computation time by applying an adapted full-multigrid (FMG) technique which is known from numerical mathematics [Stüben and Trottenberg, 1982]. The elastic FMG model also solves the problem of interactively correlating only a few homologous anatomical landmarks [Rohr et al., 1996], since the three-dimensional nonlinear deformation field results directly from the solution of a system of partial differential equations describing the unique movement (deformation) of the individual onto the reference volume for *each* voxel. This movement of the source onto the reference image is subject to constraints (Eq. 6) imposed by the continuum theory of mechanics and is therefore guided by the data per se.

The aim of the nonlinear approach is to find a transformation $\vec{x} \rightarrow \vec{x} - \vec{u}(\vec{x})$ that maps all voxels with coordinates $\vec{x} = (x_1, x_2, x_3)$ of the individual brain T onto the reference brain R by the local displacements $\vec{u} = (u_1, u_2 u_3)$. For this purpose, the volumes are modelled as an elastic medium by applying an elastic potential [Budò, 1980]

$$\Phi = -\frac{1}{2}\mu\vec{u}\Delta\vec{u} + \frac{1}{2}(\lambda + \mu) \cdot (\vec{\nabla} \cdot \vec{u})^2 \qquad (5)$$

and minimizing a squared-error distance measure $D(\vec{u})$

$$D(\vec{u}) = |T(\vec{x} - \vec{u}(\vec{x})) - R(\vec{x})|^2 \qquad (6)$$

yielding the partial differential equation

$$-\mu\vec{\Delta}\vec{u}(\vec{x}) - (\mu + \lambda)\vec{\nabla}(\vec{\nabla} \cdot \vec{u}(\vec{x}))$$
$$= 2\vec{\nabla}T(\vec{x} - \vec{u}(\vec{x}))(T(\vec{x} - \vec{u}(\vec{x})) - R(\vec{x})) \qquad (7)$$
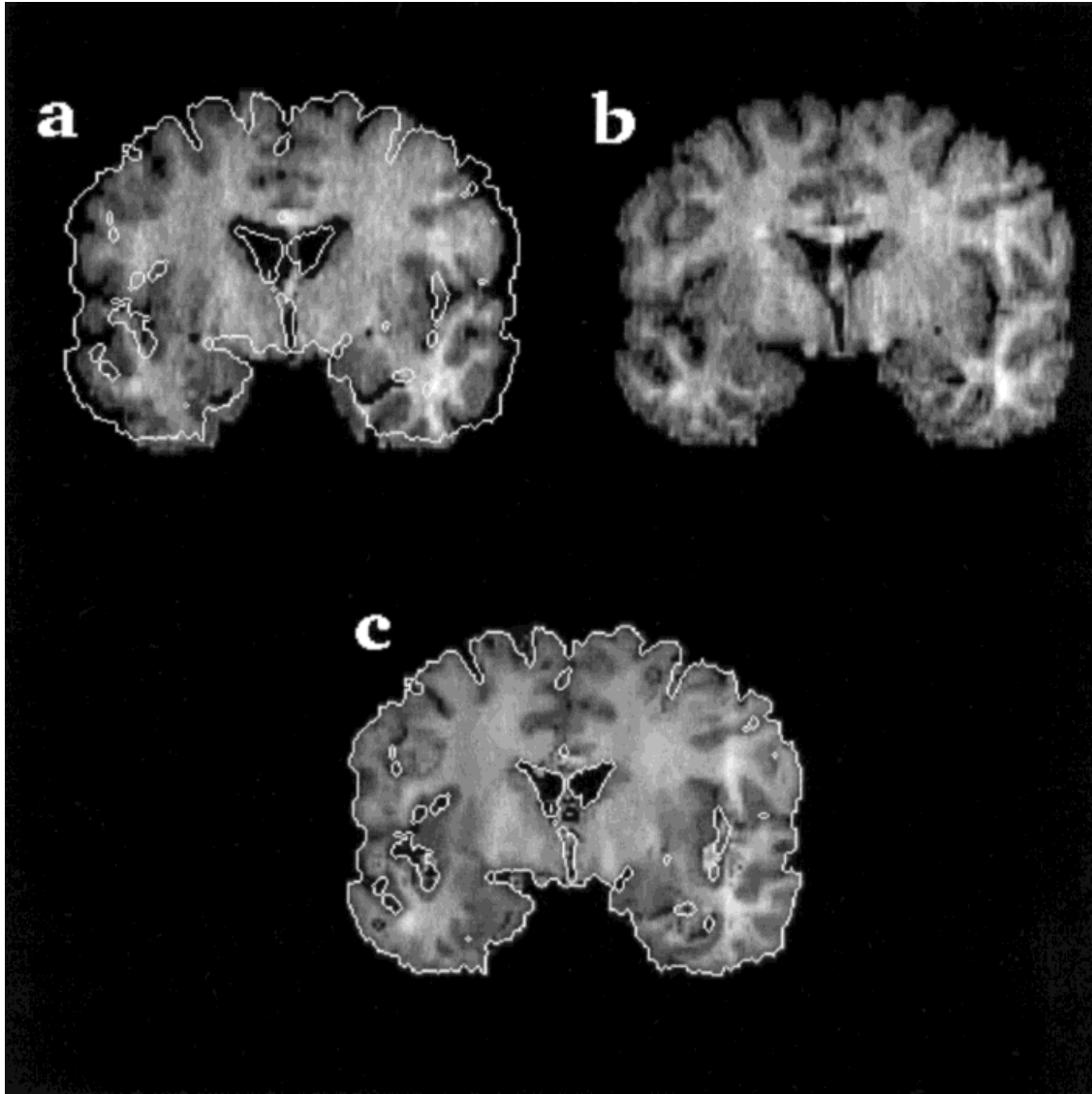
Figure 3.

Section of an individual three-dimensional brain data set with the superimposed contour of the standard brain **(b)** before **(a)** and after **(c)** three-dimensional nonlinear alignment. The outer con- tour is only used to demonstrate accuracy before and after alignment. As can be seen from the deformation field (Fig. 4), the nonlinear transformation accounts also for internal structures.

whereby $\bar{u}$ denotes the local displacements; t the transpose; μ, λ the Lamé constants; Δ, $\vec{\nabla}$ and $\bar{\nabla}\cdot$ are the Laplacian, gradient, and divergence operators, respectively.

The partial differential Eq. (7) has to be applied to each voxel of the volume by discretization, thereby working on a hierarchy of grids Ω_l^h, where Ω_0^h denotes the finest and $l = 6$ the coarsest grid in our applications. h is a discretization parameter. Thus, the discrete form of the Navier-Lamé equation applied to volumes can be written as

$$\mathrm{NLE}^h \cdot \bar{u}^h = \vec{f}^h \quad \Omega_0^h$$

$$\bar{u}^h = \vec{0} \quad \partial\Omega_0^h \tag{8}$$

where $\mathrm{NLE}^h \in \mathrm{IR}^{3 \cdot 2^{23}} \times \mathrm{IR}^{3 \cdot 2^{23}}$ is a grid operator corresponding to the finest resolution, $\bar{u}^h = (u_1^h, u_2^h, u_3^h)$ the deformation field, $\vec{f}^h = (f_1^h, f_2^h, f_3^h)$ the forces, and $\bar{u}^h = \vec{0}$
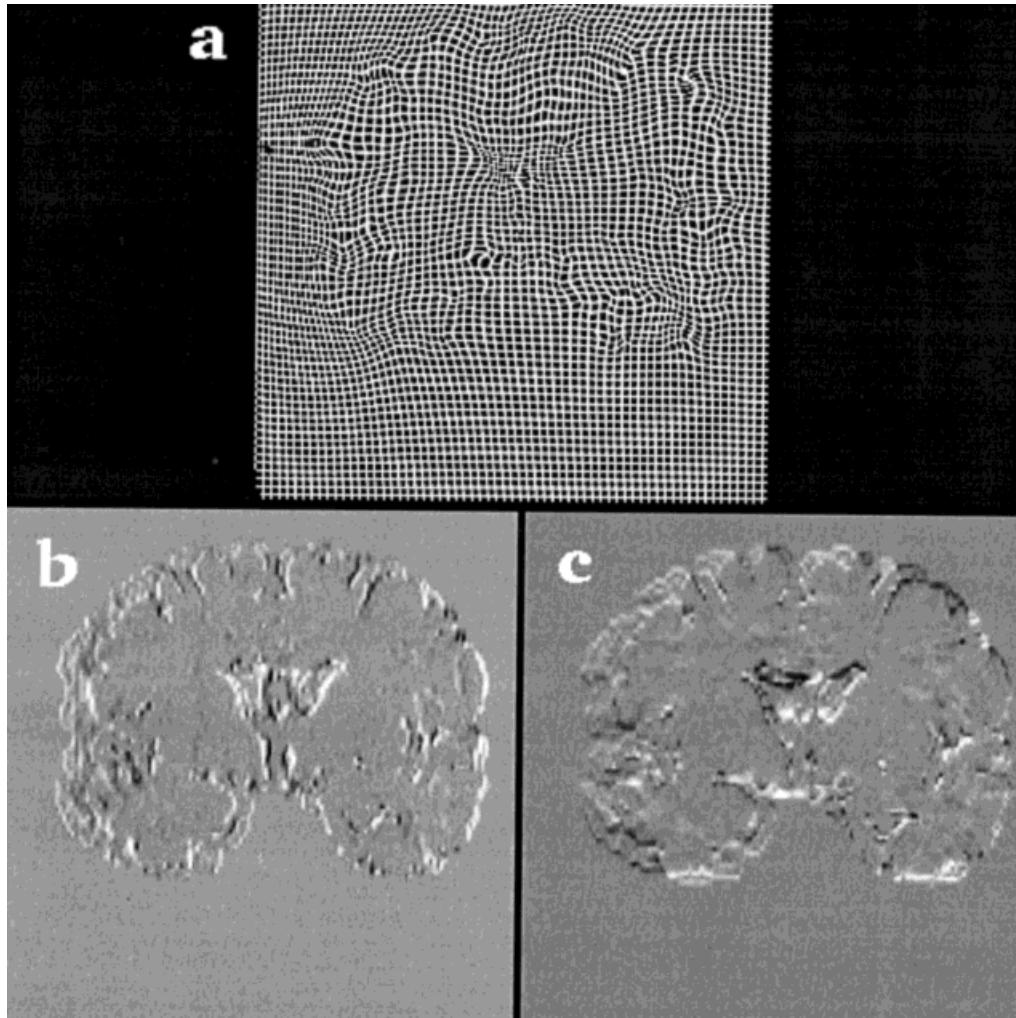
Figure 4.

a: Deformation field applied to a regular grid. The deformation field is calculated from the sections shown in Figure 3a,b. It is applied to a regular grid in order to make areas of deformation visible. The external forces for the x- **(b)** and y- **(c)** direction are shown, whereby the gray value of the background represents a force of strength zero. The direction of the force is encoded in b such that white indicates a force into the negative x-direction (black, positive x-direction), whereas white in c indicates a force into the positive y-direction (black, negative y-direction).

on $\partial\Omega_0^h$ the Dirichlet boundary condition. As an example, Figure 3 shows the iterative application of the model for 2 individuals without any interactive support, whereby the outer contour is only used to visualize the spatial differences before and after registration. The deformation field (Fig. 4a) accounts for large and complex spatial differences and results from the application of the external forces shown in Figure 4b,c for the x- and y-direction. A further example of interindividual alignment is shown in Figure 5.

Although the deformation field is derived from a system with up to 24 million degrees of freedom, the resulting transformation is unique, since the movement (deformation) of the brain is a consequence of applying the variational principle of Hamilton to an elastic potential known from the theory of continuum mechanics and a distance measure thereby introducing *the same number of constraints*. Thus, after by applying Dirichlet boundary conditions, the system of partial differential equations is uniquely determined and solved precisely, i.e., within a selected numerical accuracy of 10^{-2} by the full-multigrid method for each voxel and for a given initial position, which is also uniquely determined in a first step by the extended
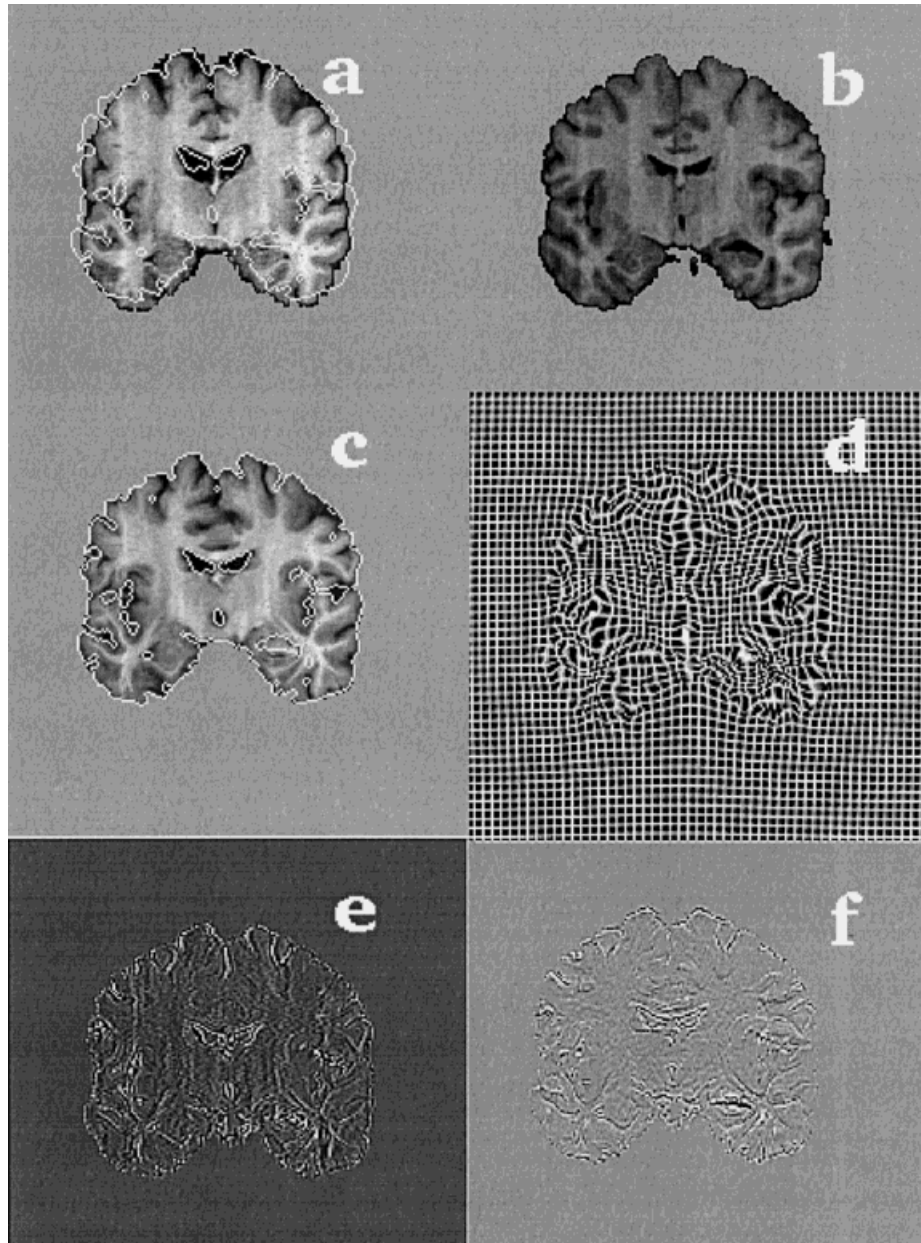
Figure 5.
Example of a two-dimensional interindividual alignment. Source image before **(a)** and after **(c)** nonlinear alignment, with reference section **(b)**. **d:** Deformation field. **e,f:** Forces for the x- and y-directions, resepctively. Computation time for this example was approximately 20 sec on a SUN SPARC20 workstation.

PAT. Another advantage of the FMG is that the numerical effort increases only linearly with O(N), N being the number of grid-points.

In addition to these physical and mathematical aspects, there are in principle possible constellations of corresponding objects (e.g., infinite periodical structures) for which an automatic alignment would lead to different results, e.g., depending on the relative position before nonlinear transformation. Also, misregistration may be introduced according to Eq. (6) in cases where homologous structures in reference and source volumes do not overlap (e.g., corresponding gyri). However, due to the fact that the algorithm is additionally embedded in a multiresolution framework, i.e.,

alignment follows stepwise, from a coarse to a fine registration, the correlation of homologous structures is greatly improved, even when morphology is complex such as in the human brain. It has to be mentioned that further characterizations are required with respect to the gray-value-dependent convergence and the uniqueness of this complex algorithm, on which we are currently working.

CONCLUSIONS

A technique has been developed for integrating microscopical and MR information, in order to improve the mapping of specific brain structures with respect to their identification and localization, which can be used in combining functional and morphological data. Research was focused mainly on the development of a system which provides high accuracy with minor interactive support and minimization of computation time. This was achieved by a hierarchical technique which is based on an extended principle axes theory (PAT) generalized to affine parameters and a three-dimensional high-dimensional transformation determined by a fast full-multigrid method (FMG). With this technique it is possible to account for the global alignment required for the high-dimensional transformation as well as for the different morphology with complex neuroanatomical shape. In addition, a combination of the PAT and the FMG method is used for an accurate three-dimensional reconstruction of histological volumes.

REFERENCES

Bajcsy R, Kovacic S (1989): Multiresolution elastic matching. Comput Vision Graph Im Proc 46:1–21.

Bro-Nielsen B, Gramkow C (1996): Fast fluid registration of medical images. Lecture Notes Comput Sci 1131:266–276.

Broit C (1981): Optimal registration of deformed images. Philadelphia: University of Pennsylvania. Doctoral dissertation.

Budò A (1980): Theoretische Mechanik, Berlin: Verlag der Wissenschaften.

Christensen GE, Rabbitt RD, Miller MI (1994): 3-D brain mapping using deformable neuroanatomy. Phys Med Biol 39:609–618.

Cygansky D, Orr JA (1985): Application of tensor theory to object recognition and orientation determination. IEEE Trans Pattern Anal Mach Intell 7:662–673.

Faber TL, Stokeley EM (1988): Orientation of 3-D structures in medical images. IEEE Trans Pattern Anal Mach Intell 20:626–633.

Landau LD, Lifshitz EM (1959): Theory of Elasticity, London: Pergamon Press.

Miller MI, Christensen GE, Amit Y, Grenander U (1993): Mathematical textbook of deformable neuroanatomies. Proc Natl Acad Sci USA 90:11944–11948.

Rohr K, Stiehl HS, Sprengel R, Beil W, Buzug TM, Weese J, Kuhn MH (1996): Point-based elastic registration of medical image data using approximating thin-plate splines. Lecture Notes Comput Sci 1131:297–307.

Roland PE, Zilles K (1994): Brain atlases—A new research tool. TINS 17:458–467.

Schormann T, Zilles K (1997): Limitations of the principle axes theory. IEEE Trans Med Imaging 16:942–947 .

Schormann T, von Matthey M, Dabringhaus A, Zilles K (1993): Alignment of 3-D brain data sets originating from MR and histology. Bioimaging 1:119–128. Erratum, Bioimaging 1:185.

Schormann T, Dabringhaus A, Zilles K (1995): Statistics of deformations in histology and improved alignment with MRI. IEEE Trans Med Imaging 14:25–35.

Schormann T, Henn S, Zilles K (1996): A new approach to fast elastic alignment with applications to human brains. Lecture Notes Comput Sci 1131:337–342.

Schormann T, Dabringhaus A, Zilles K (1997): Extension of the principal axes theory for the determination of affine transformations. In: Paulus E, Wahl FM (eds): Proceedings of the DAGM: Informatik Aktuell. Berlin: Springer-Verlag, pp 384–391.

Stüben K, Trottenberg U (1982): Multigrid methods: Fundamental algorithms, model problem analysis and applications. In: Hackbusch W, Trottenberg U (eds): Multigrid Methods. Lecture Notes in Mathematics, Volume 960. Berlin: Springer-Verlag.